

DESIGN OF QUASI-TRAVELING WAVE PINGER MAGNET FOR BEAM DIAGNOSTICS ON THE ADVANCED LIGHT SOURCE

D.E. Anderson and G. Stover , Lawrence Berkeley National Laboratory, 1 Cyclotron Rd., Berkeley, CA 94720

Abstract

A beam diagnostic tool to modify single bunch orbits in all four quadrants is proposed for measuring various machine physics parameters at the Advanced Light Source (ALS). Quasi-Traveling Wave pinger magnets were chosen to provide programmable bipolar horizontal and vertical kicks of sufficient duration while providing negligible deflection on subsequent beam revolutions in the storage ring. This magnet technology, originally investigated at the SSC[1], provides a cost-effective method of achieving the moderately fast pulse requirements of the pinger application. The design of the pinger magnet and associated pulsed power drive unit will be presented. Electrical response results of initial pinger magnet prototypes and ceramic beampipe coatings will be given.

1 INTRODUCTION

An orthogonal set of horizontal and vertical fast kicker magnets and their requisite pulse forming networks, termed the "pinger" system, are currently being constructed for installation in the ALS storage ring. The pinger system was specifically designed to apply a single one turn kick to an orbiting bunch in the storage ring. The kick is intended to provide an independently adjustable change in the single bunch's transverse momentum. Following the kick, 1024 subsequent turns of transverse bunch motion can be captured by an existing circumferential array of 96 BPM's operating in the "fast acquisition data" mode.

Comparison of actual bunch motion orbits with computer simulations should provide improved parameter definition for the model and refine measurements of critical machine parameters that should lead to improved storage ring performance. The necessary parameters to accomplish this task are shown in table I below.

Table I—Pinger Magnet System Parameters

Horizontal Bdl Kick	$\pm 2.5-157.5$ Gauss-m
Vertical Bdl Kick	$\pm 6.25-80$ Gauss-m
Magnet Aperture	91mm \times 91mm
Magnet Length	475mm V&H
Field Uniformity	$\pm 5\%$
Pulse flattop duration	≥ 25 ns
Post-pulse Oscillations	$\leq \pm 1\%$ B_{max} after 650ns

2 MAGNET TECHNOLOGY OPTIONS

Various magnet technologies were considered to meet the requirements for the pinger application. C-magnets and window-frame magnets were considered and compared. System topologies considered included lumped inductance, 1% underdamped series RLC, traveling-wave, and quasi traveling-wave. In an effort to minimize system cost and complexity, it was desirable to build each horizontal and vertical kicker with a single 475 mm magnet and to maintain operating voltages below 35 kV (single-gap thyratron).

1.1 C- vs. Window-frame magnets

Window-frame magnets, with a septum decoupling the two halves of the magnet, are advantageous in reducing the overall magnet inductance when the two halves are driven in parallel. However, this magnet type becomes an integral part of the beam line once installed, since removal of the magnet requires complete disassembly of the magnet. C-magnets can be removed from the beam line with a minimal effort by removing the return conductor plate and sliding the assembly away from the beampipe.

1.2 System topology considerations

Lumped inductance magnets were considered first because of their relative simplicity. A peak operating voltage of 35kV with a current peak of 2400A dictates a maximum driving impedance of 7.3 Ω . An impedance of 6.25 Ω was chosen to maintain charge voltages at 30kV and still allow for operation 10% over specification. At this impedance level with a 600nH kicker magnet inductance, the time constant is 96ns, making any flattop unachievable.

An underdamped RLC circuit, allowed to reverse 1% within the 650ns post-pulse oscillation period, was also considered. The condition for this case is $R=1.7(LC)^{0.5}$. Circuit simulations were run to determine the system topology. The inductance and capacitance of the cables connecting the magnet to the pulser were found to have a profound effect on the circuit performance. A solution was found which used a 3 Ω cable, but post-pulse ringing in the cable was $\sim 5\%$, and thus deemed unacceptable.

Traveling-wave magnets were investigated, and could easily meet the system parameters. Their high

manufacturing cost made them unattractive, so other alternatives were investigated.

Quasi traveling-wave magnets, consisting of a lumped ferrite magnet with shunt capacitors placed along its length, approximates a transmission line, and thus should produce a moderately fast risetime with minimal reflections. The magnet topology is shown in Figure 1. The risetime is limited by some percentage of the magnet inductance (which is a function of the number of discrete capacitors incorporated) which the forward-going pulse initially sees upon arrival at the magnet.

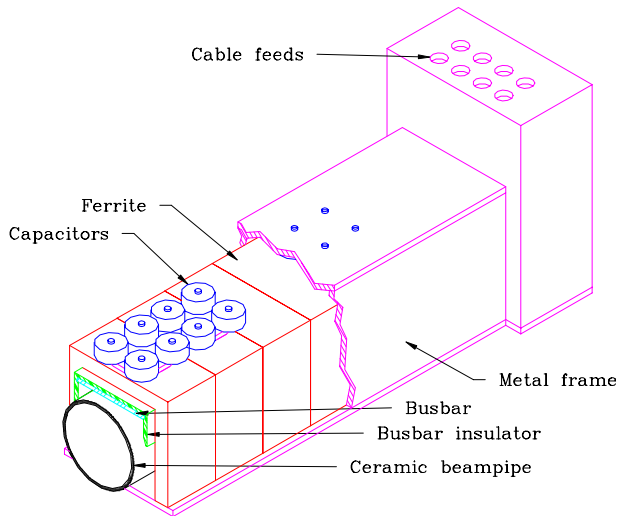


Figure 1—Quasi Traveling-Wave Pinger Magnet Geometry. Load not shown for clarity.

3 PINGER SYSTEM DESIGN

Design of the pinger system is closely coupled to the design of the magnet. The initial inductance seen by the forward-going wave as it arrives at the magnet affects the risetime of the $\int Bdl$ signal and subsequent post-pulse reflections. These effects influence the choice of number of stages in the quasi traveling-wave magnet, the length of the cable isolating the pulser from magnet and the pulse-forming network (PFN) topology.

The forward-going wave, upon arriving at the magnet, is partially reflected back toward the pulser by the initial magnet inductance. After transiting through the cable and PFN, the reflected energy is then transformed into $\int Bdl$ signal following the main pulse. To first-order, the sum of the two-way transit times through the magnet to pulser cable and PFN is equal to the bunch transit time in the ring minus the risetime of $\int Bdl$ (the duration of the reflected pulse). To maintain post-pulse levels below 1% in the pinger application, this resulted in a three section magnet with 120ns and 100ns one-way cable and PFN transit-times, respectively, in the optimized system. Figure 2 shows the system schematically.

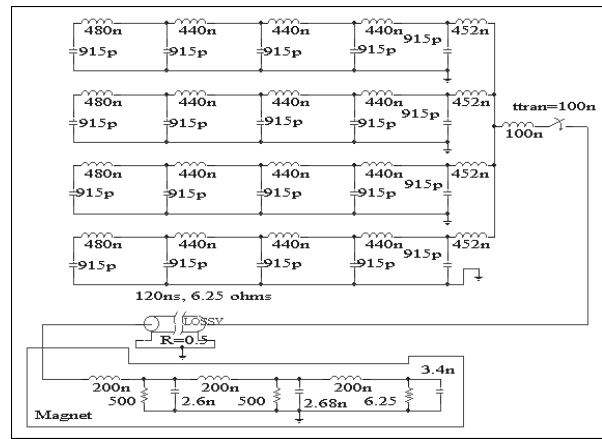


Figure 2—Pinger System Schematic used in Circuit Simulations

The inclusion of a resistively-coated ceramic beampipe is necessary to carry beam return currents in a low-impedance configuration. The high resistivities required for magnetic field diffusion into the beampipe result in moderate power dissipation generated by the beam image currents. The penetration time constant, given by $\tau_p = 2\pi a/R$ ns, where a is the pipe radius in cm and R is the surface resistivity (Ω/\square), must be much less than the risetime of the external magnetic field[2].

The permitted $\pm 5\%$ variation in field over the duration of the flattop of the pulse permitted the use of a pulse-forming network for driving the magnetic field. The ability to “float” the PFN also allowed for a relatively low inductance output structure, an important feature to achieve sub-100ns risetimes at 6.25 Ω impedance. Bipolar operation is achieved through the use of two identical PFNs connected to the same switch. The unutilized PFN is shorted and connected to ground, thereby referencing the anode or cathode of the thyatron to ground. The PFN outputs are connected, via a high-voltage custom SPST switch on a 6.25 Ω stripline transmission line, to a common set of output connectors. Cables then feed into one of two π -network high-voltage stripline attenuators. Use of these attenuators allows for vertical and horizontal low and high range operation with the same pulser units.

The remote connection to the ALS computer control system is accomplished through the standard Intelligent Local Controller (ILC)[3] module. The module is connected to the control system via standard 422 serial fiber optic link. All analog and digital controls and monitors are provided by the ILC. All digital and +24V chain signals to and from the pinger are also optically isolated from the ILC.

Basic trigger timing (Storage Ring Orbit Clock) will be transmitted to the pinger racks via fiber optics. Trigger delay control will be provided by a commercial timing delay generator controlled through an IEEE interface to the ILC.

4 PROTOTYPE RESULTS

To verify the suitability of a quasi-traveling wave magnet for the pinger application, a prototype magnet was built and tested. The prototype used Stackpole C11 NiZn ferrite, had an 88mm×88mm aperture, and was 530mm long. Ceramic doorknob capacitors were located equally-spaced at three locations on the structure. The ALS kicker magnet test stand, an 8.33Ω system with 20ns risetimes, was used to drive the 6.25Ω pinger magnet through a 6dB attenuator/impedance-matching π network. This prototype magnet was used to measure the electrical response of quasi-traveling wave magnets and to quantify penetration time effects of resistively-coated beampipes.

4.1 Electrical response of prototype magnet

A 50Ω stripline B-dot probe, 600mm long, was constructed to monitor the magnetic field in the magnet. The signal generated was then integrated using the digitizer integration package. The result for the prototype magnet is shown in Figure 3.

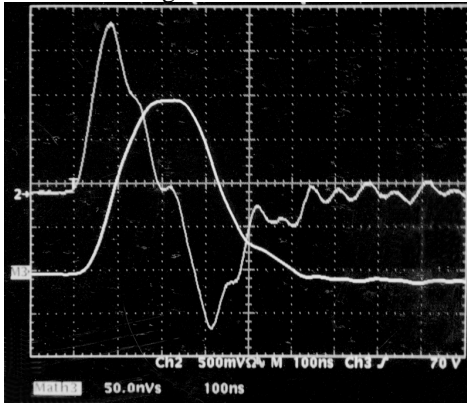


Figure 3—Pinger Magnet Prototype Electrical Response. Signals are a) direct B-dot signal and b) software integrated $\int B \cdot dl$ (pulse).

The magnet produced an $\int B \cdot dl$ risetime (10-90%) of 120ns, with 53ns of flattop at $\pm 0.5\%$. The calculated one-way transit-time through the magnet of 107ns agrees well with the measured risetime minus the input pulse risetime. The poor falltime with the long “foot” is due to the energy reflected off the magnet after returning from the PFN. The peak value of the dB/dt signal agrees well with that expected for the calculated magnetic gain at the measured dI/dt .

A higher impedance magnet structure was also tested. This 8.33Ω magnet, with identical physical dimensions, was also pulsed. The risetime was reduced to 106ns, which agrees well with the 80ns one-way transit-time through the magnet. Other aperture size magnets were also tested with predictable results.

4.2 Beampipe coating and penetration measurements

The inside surface of the ceramic vacuum chamber (137mm length and 72mm dia.) was coated with thermally sublimed titanium in a nominal vacuum of 6×10^{-6} Torr. The coating process was driven to an estimated center tube resistivity of $2.0 \Omega/\square$. The actual longitudinal resistivity profile was parabolic in form. Thus the average resistivity for the total tube was measured at $2.7 \Omega/\square$. This value was chosen to minimize excessive eddy current shielding effects of the fast rising (100ns) magnet field and reduce the thermal heating of the tube from beam image currents. Calculations indicate a maximum of 110 watts will be dissipated in the tube at nominal storage ring energies and currents.

Magnetic field penetration measurements were performed on the 6.25Ω magnet using the stripline B-dot probe. Figure 4 shows the measured waveforms for various resistivity coatings.

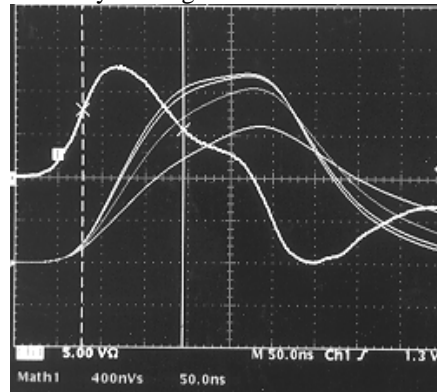


Figure 4— $\int B \cdot dl$ for Various Resistivity Beampipe Coatings. Beampipe I.D. 60.3mm with a) infinite Ω/\square ($\tau_p=0$), b) $1.941 \Omega/\square$ ($\tau_p=9.8$ ns), c) $0.572 \Omega/\square$ ($\tau_p=33.1$ ns), and d) $0.180 \Omega/\square$ ($\tau_p=105.2$ ns) coating resistivities.

REFERENCES

- [1] D. Anderson and L. Schneider, “Design and Preliminary Testing of the LEB Extraction Kicker Magnet at the SSC”, *Proceedings of the 1993 Particle Accelerator Conference*, May 1993, pp.1354-6.
- [2] Peterson, J.M., “Requirements for Resistive Coating on Ceramic Tubes in Kicker Magnets”, *Single Pass Collider Memo CN-49*, April 1981.
- [3] Magyary, S. and et al, “The Advanced Light Source Control System”, LBL-28412, LSEE-067.